Saudi Journal of Biological Sciences 29 (2022) 3759–3771

Contents lists available at ScienceDirect

Saudi Journal of Biological Sciences

journal homepage: www.sciencedirect.com

Original article

Recycling rice straw ash to produce low thermal conductivity and moisture-resistant geopolymer adobe bricks

Mohamed I. Morsy [a], Khaled A. Alakeel [b,*], Ahmed E. Ahmed [c,d], Ahmed M. Abbas [c,e], Abdelaziz I. Omara [f], Nader R. Abdelsalam [g,*], Haitham H. Emaish [h,*]

[a] Department of Agricultural & Biosystem Engineering, Faculty of Agriculture, Alexandria University, P.O. Box 21545, Alexandria, Egypt
[b] National Center of Agricultural Technology, Life Science & Environmental Research Institute, King Abdulaziz City for Science and Technology, Riyadh, Saudi Arabia
[c] Biology Department, College of Science, King Khalid University, 61413 Abha, Saudi Arabia
[d] Department of Theriogenology, Faculty of Veterinary Medicine, South Valley University, 83523 Qena, Egypt
[e] Botany and Microbiology Department, Faculty of Science, South Valley University, 83523 Qena, Egypt
[f] Department of Agricultural & Biosystem Engineering, Faculty of Agriculture, Alexandria University, P.O. Box 21545, Alexandria, Egypt
[g] Agricultural Botany Department, Faculty of Agriculture (Saba Basha), Alexandria University, 21531 Alexandria, Egypt
[h] Department of Soils and Agricultural Chemistry, Biosystem Engineering, Faculty of Agriculture (Saba Basha), Alexandria University, P.O. Box 21531, Alexandria, Egypt

ARTICLE INFO

Article history:
Received 3 February 2022
Revised 12 February 2022
Accepted 27 February 2022
Available online 4 March 2022

Keywords:
Adobe bricks
Compressive strength
Geopolymer
Thermal conductivity
Water absorption

ABSTRACT

Rice straw ash (RSA) geopolymer adobe bricks were produced using the geopolymerization reaction among the RSA, soil, and alkaline activator at the Biosystem Engineering Department, Faculty of Agriculture, Alexandria University, Egypt, to optimize adobe brick advantages. The bulk density, water absorption, compressive strength, and thermal conductivity of the new composite were measured at RSA contents of 0%, 5%, 10%, and 20% and sodium hydroxide contents of 2.5%, 5%, 7.5%, and 10% after curing the composite for 28 days. Results indicated that increasing RSA from 0% to 20% increased the compressive strength and decreased the bulk density, water absorption, and thermal conductivity. Further, increasing sodium hydroxide from 2.5% to 10% increased the bulk density and compressive strength and decreased the water absorption. Significant effects of RSA and sodium hydroxide percentages and their interaction on all the studied characters were reported. The best conditions to minimize bulk density, water absorption, thermal conductivity, and optimize compressive strength of the composite were at 10% sodium hydroxide and 20% RSA. The minimum bulk density, water absorption, and thermal conductivity were 1.463 g/cm^3, 8.3%, and 0.46 W/(m·K), respectively, while the maximum CS was 2.1 MPa after 28 days. Using RSA geopolymer adobe bricks on building interior walls is recommended to decrease bricks' thermal conductivity, water absorption, and weight.

1. Introduction

Rice straw is an important agricultural waste that causes environmental problems if not properly used, such as field burning, which increases air pollution and methane emission. Furthermore, the straw is a hazardous source of fires because farmers store it on rooftops. (Yuan et al., 2014, Bamminger et al., 2018; Buyondo et al., 2020; Nan et al., 2020). However, the straw is used for feeding animals, mushroom farming, and biofuel production (Foaud and Abdelradi, 2016; Babé et al., 2020; Mohamed and Morsy, 2018, 2020; Hassan et al., 2021; Phuong et al., 2021). Rice straw ash (RSA) is the main source of silica (87–97%) used as a building material. The ash is obtained by burning the rice straw in an incinerator under controlled burning temperatures of 600–700 °C (Kalapathy et al., 2002; Li et al., 2004). Building materials are responsible for 36% of the carbon dioxide (CO_2) emissions and 40% of the energy consumption in the European Union. Portland cement is a high energy consumption building material and generates large amounts of CO_2. The production of 1 kg of ordinary Portland cement consumes about 1.5 kW h of energy and releases about 1 kg of CO_2. Worldwide, the production of ordinary Portland

* Corresponding authors.
E-mail addresses: kaalakeel@kacst.edu.sa (K.A. Alakeel), nader.wheat@alexu.edu.eg (N.R. Abdelsalam), drhaitham1976@alexu.edu.eg (H.H. Emaish).

Peer review under responsibility of King Saud University.

Production and hosting by Elsevier

https://doi.org/10.1016/j.sjbs.2022.02.046
1319-562X/

cement is responsible for about 7% of all CO_2 emissions. Manufacturing eco-friendly building materials is urgent to decrease climate change, energy consumption and natural resources. New studies have improved advanced technology in cement production to decrease CO_2 emissions using natural geopolymer binders (Habert et al., 2010; Habert et al., 2011; Gunasekara et al., 2018; Nanayakkara et al., 2021). The geopolymer materials were invented in 1979 by the alkaline activation of mud and soil materials. It has been a great development in this field since this time. Many researchers have studied alkaline activated materials (geopolymers) from different directions, related reactions, influencing factors, and the resulting material properties (Jullien et al., 2012; Dirgantara et al., 2017; Khodr et al., 2020). Geopolymer composites have attracted the attention of researchers to replace Portland cement by the alkaline activation of alumina and silica-rich materials using alkaline activators such as sodium silicate and sodium hydroxide solutions (Li et al., 2004). The alkali-activated aluminosilicate materials have many advantages of water insolubility, excellent mechanical properties, compact microstructure, resistance to aggressive solutions, high temperatures (up to 120 °C), and brisk temperature changes and do not produce hazardous gaseous components during thermal exposure (Hansen and Boegh, 1985; Jiang et al., 2014; Tome et al., 2021; Zhang et al., 2021). Increasing RSA in geopolymer concrete increased the durability of the new composite, but an additional source of aluminum is needed because RSA contains very little aluminum (Piyaphanuwat and Asavapisit, 2009; Thomas et al., 2021). Bricks are an important building material; they are usually made of clay and require a high temperature of 900–1000 °C. The high kiln firing temperature consumes a large amount of energy and releases large quantities of harmful gases (Ahmari and Zhang, 2012; Buyondo et al., 2020). Concrete bricks are produced from ordinary Portland cement and aggregates, which requires high energy consumption and releases large amounts of harmful gases (Arshad and Pawade, 2014; Kubiś et al., 2020; Kurmus and Mohajerani, 2021). Adobe brick is one of the most important and ancient building materials used all over the world. It is made by mixing organic material, mud, water, straw, or other fibers that can be added to increase composite strength (Trang et al., 2021). In high-temperature regions, using adobe bricks in buildings offers many advantages, such as being durable, fireproof, non-toxic, biodegradable, low thermal conductivity, and low sound transmission levels through walls (Babé et al., 2020; de Castrillo et al., 2021; Ige and Danso, 2021). Lightweight bricks are better than normal bricks because they are easy to handle and reduce the transportation cost (Piyaphanuwat and Asavapisit, 2009). The thermal conductivity of adobe brick describes how easily heat flows through the brick material. Adobe bricks with low thermal conductivity are suitable for thermal insulation because heat will transfer slowly through the material (Kubiś et al., 2020; Hany et al., 2021; Kurmus and Mohajerani, 2021). This study aims to develop new geopolymer adobe bricks using RSA wastes as soil stabilizers, determine their mechanical, physical, and thermal properties, and decrease the thermal conductivity, water absorption, and weight of the RSA geopolymer adobe bricks.

2. Materials and methods

In this study, RSA and soil samples were the main components for manufacturing low thermal conductivity and moisture-resistant geopolymer adobe bricks. The soil sample was used as the base material. At the same time, RSA and sodium hydroxide was added in different percentages to study the changes in the compressive strength (CS), density, thermal conductivity, and water absorption of the geopolymer adobe bricks.

2.1. Materials

RSA geopolymer adobe brick is manufactured using the following materials. After harvesting a rice crop from El Hamam Experiment Station, Faculty of Agriculture, Alexandria University, Egypt, the rice straw was collected. The RSA was obtained by burning the rice straw in an incinerator at 600 °C, as described by (Kalapathy et al., 2002). The RSA color is dark gray, as shown in Fig. 1a. The soil sample was collected from El Hamam Experiment Station, Faculty of Agriculture, Alexandria University, Egypt, as shown in Fig. 1b and c. The soil sample was taken from the top layer 10 cm using a shovel and placed in polyethylene bags. Clean tap water was used in this study with 50% of the total weight of the soil sample and RSA. The alkaline solution was a combination of sodium silicate and sodium hydroxide solutions with a ratio of 2.5:1 sodium silicate to sodium hydroxide, purchased from a local supplier. The sodium silicate solution (Na_2SiO_3) comprises Na_2O = 13.7%, SiO_2 = 29.4%, and water = 55.9% by mass. The alkaline solution was prepared by dissolving the sodium silicate and sodium hydroxide in 500 g water for each sample of Adobe bricks.

2.2. Methodology

The chemical composition of RSA was determined using the X-ray fluorescent elemental analyzer (EA-XRF, Dandong, Liaoning, China) (Khorsand et al., 2013) as presented in Table 1. The true density of RSA was determined using a helium pycnometer (Berger, 2010). The particle size analysis for RSA was performed using a set of 300, 225, 150, 100, 75, and 50 μm sieves. The set of sieves was placed on a shaker for 15 min. The weights of RSA retained on each sieve were measured. The sieve analysis results are shown in Fig. 2.

2.3. Composition of geopolymer adobe bricks

The RSA geopolymer adobe bricks were manufactured using RSA, natural soil, sodium hydroxide, sodium silicate, and water in a mix of 1500 g (Gavali et al., 2021). The used mixture proportions of geopolymer are shown in Table 2. Batching of materials was done by weight. The replacement percentages of soil by RSA were 5%, 10%, and 20%. The 0% RSA was considered a reference sample for the other samples. The ratios of an alkaline solution to the binder were 2.5%, 5%, 7.5%, and 10% of the total weight of natural soil and RSA, and the ratio of water to binder (w/b) was about 50% (Bondar et al., 2011).

2.4. Experimental procedures

The experimental design was conducted as factorial experiments in two factors: the first factor was rice straw ash of 0%, 5%, 10%, and 20%, and the second factor was the ratios of sodium hydroxide of 2.5%, 5%, 7.5%, and 10%. Each treatment was distributed across three replications.

2.4.1. Preparation of test specimen

The materials for the used mixture were weighed and mixed in a dry condition for 5 min. The sodium hydroxide and sodium silicate solutions were added to the dry mix and stirred for 10 min. The obtained geopolymer was poured in a 40 × 40 × 160 mm^3 mold as shown in Fig. 3. The specimens were placed in the oven at 80 °C for 24 h. Then, the specimens were removed from their molds. One-half of the specimens were cured at room temperature for 28 days, while the other half was immersed in water for 28 days.

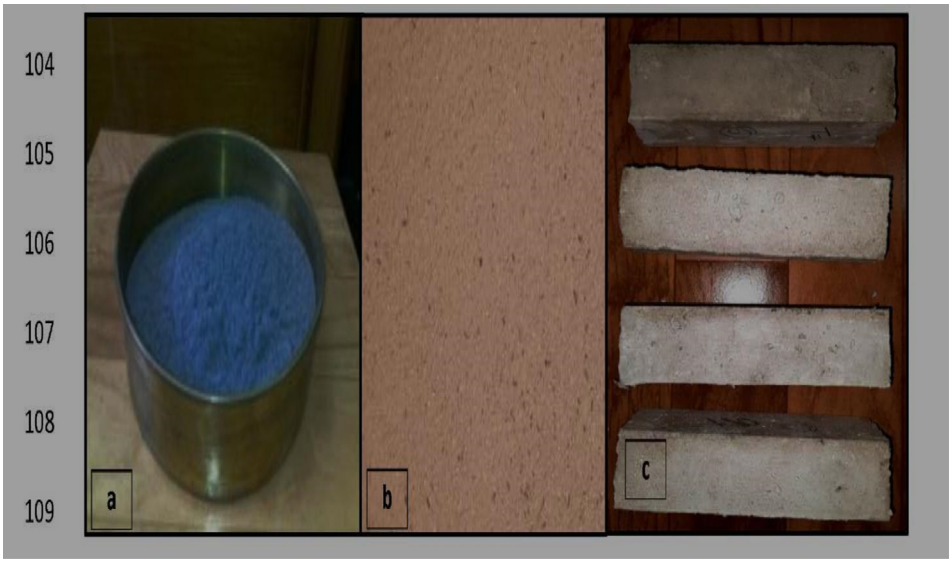

Fig. 1. (a) Rice straw ash, (b) soil sample and (c) RSA geopolymer adobe bricks.

Table 1
The elemental composition (wt%) of rice straw ash used in this study determined using X-ray fluorescence.

Constituent	Fe_2O_3	SiO_2	CaO	Al_2O_3	MgO	K_2O	Na_2O	SO_3	L.O.I.
Rice straw ash	0.9	69.2	3.46	5.3	2.81	6.4	3.43	0	8.5

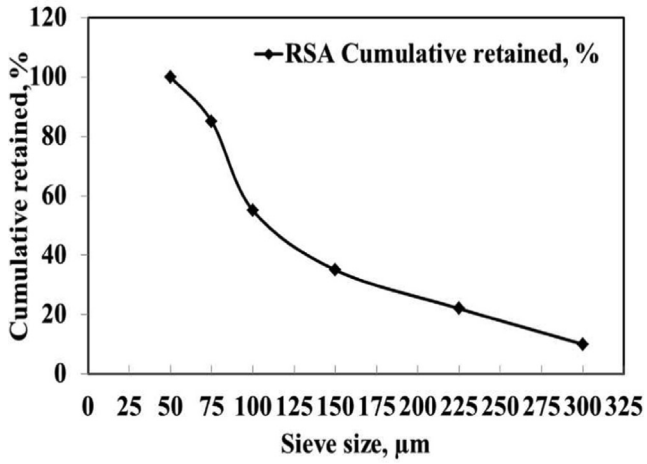

Fig. 2. Rice straw ash particle size analysis.

2.4.2. Mechanical tests

The compressive strength (CS) of the RSA geopolymer was tested according to the European Standard (DIN EN 196-1). A servo-hydraulic material testing system with a maximum capacity of 100 kN was used to apply a constant loading rate test of 140 kg/(cm min) until failure. A specimen of dimensions 40 × 40 × 160 mm^3 was used for each test. Three replicates of CS tests were applied on specimens of different RSA contents, as given in Table 2**.** After 7 days and 28 days of removing the specimen from the mold, the tests were conducted. The CS was calculated as follows:

$$CS = \frac{Fu}{W^2}$$

where CS**:** Compression stress, MPa; Fu**:** Ultimate load, N; and W**:** Width of the sample, mm (ASTM, 1950).

2.4.3. Physical properties

2.4.3.1. A. Bulk density. For determining the bulk density of hardened composites, a set of samples, each of dimensions 40 × 40 × 160 mm^3, were tested. Three replicates of each sample were tested after 28 days from removing from the mold. All samples were dried at 105 ± 5 °C until a constant weight was achieved and then were placed in the air to cool. The weight and volume of each dried specimen were measured. The bulk density was determined as follows:

$$\rho b = \frac{W_d}{V}$$

where ρb**:** Sample bulk density, g/cm^3; W_d**:** Weight of dry sample, g; and V**:** Volume of the sample, cm^3 (ASTM, 1950).

Table 2
Mixture proportions of RSA geopolymer adobe bricks.

Experimental	Natural soil (g)	RSA (g)	NaOH (g)	Water (g)
100% Soil, 0% RSA	1000	0	25, 50, 75, & 100	500
95% Soil, 5% RSA	950	50	25, 50, 75, & 100	500
90% Soil, 10% RSA	900	100	25, 50, 75, & 100	500
80% Soil, 20% RSA	800	200	25, 50, 75, & 100	500

RSA: Rice straw ash.

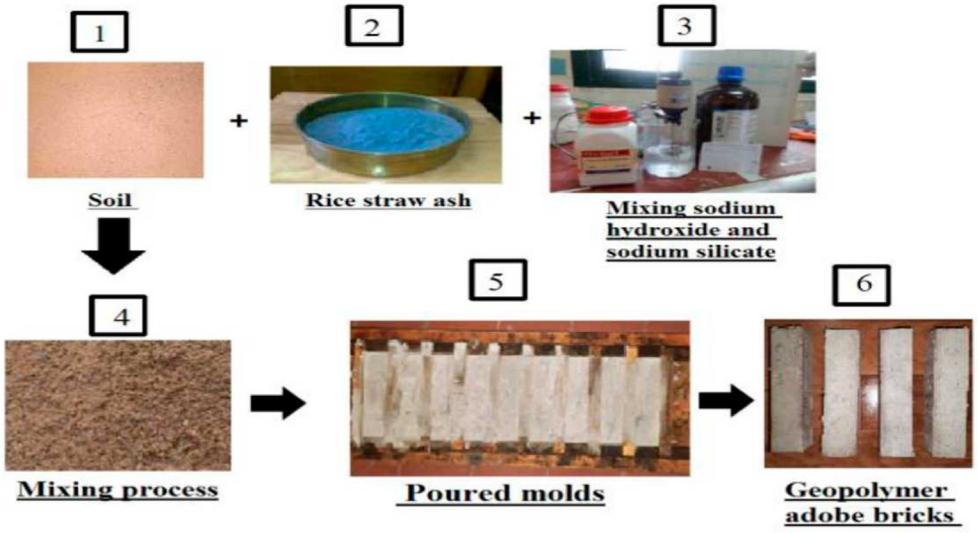

Fig. 3. Rice straw ash geopolymer adobe brick production steps.

2.4.3.2. Water absorption. Three replicates were used for each test after 28 days to determine water absorption. All samples were dried at 105 ± 5 °C until achieving a constant weight. Water absorption was determined using the American Standard Testing Method ASTM (D-1037): the dried specimens were weighed to the nearest 0.01 g. The tested specimens were then soaked in water at room temperature for 24 h. The specimens were hung to drain the water for 10 min and the excess surface water was wiped off and then were weighed to the nearest 0.01 g. The amount of absorbed water after 24 h was calculated as a percentage of the original weight of test specimens.

$$W = \left(\frac{W_a - W_d}{W_d}\right) \times 100$$

where W: Water absorption, %; W_a: Weight of saturated sample in air, g; and W_d: Specimen dry weight, g (ASTM, 1950).

2.4.4. Thermal conductivity

The thermal conductivity is the time for an amount of stable heat flow (watts) through the unit area (m^2) per temperature unit of a gradient in the perpendicular direction to an isothermal surface, which is expressed in watts per meter per kelvin (W/(m·K)). The thermal conductivity of hardened RSA geopolymer adobe brick was measured after 28 days with a quick thermal conductivity meter using the hot-wire method with a range of 0.023–12 W/(m·K) and precision of ±5% (ASTM, 1950; Alvarado et al., 2012).

2.4.5. Scanning electronic microscope (SEM)

A scanning electron microscope (JSM-5300; JEOL, Japan) was used to investigate the soil structure, RSA, and RSA geopolymer adobe brick. The samples were gold sputter-coated before analysis and the microscope was operated at 20 kV, as described by Ismail et al. (2016) and Capson-Tojo et al. (2020).

2.4.6. Ftir spectrometer

The FTIR spectrometer (Perkin-Elmer BX2) was used to identify the type of molecular motions and bonds or functional groups present in the soil, RSA, and RSA geopolymer adobe bricks. The samples were scanned between the wavelengths of 400 cm^{-1} and 4000 cm^{-1} with a resolution of 4 cm^{-1}. The spectra data generated were analyzed using irAnalyze-PAMalyze 4.0 software and the organic functional groups present in the samples were characterized, as described by Nanda et al. (2013) and Yusuf et al. (2020).

2.5. Statistical analysis

All collected data were subjected to analysis of variance using the technique of Gomez and Gomez (1984). All statistical analyses were performed using the (Duncan, 1955) computer software package.

3. Results

3.1. Characterization of raw materials

The soil texture is sandy clay loam (70% sand, 8% silt, and 22% loam), with a bulk density of 1.35 g/cm^3 and a field capacity of 24.33%. The particle size analysis for RSA was performed as shown in Fig. 2, and the chemical composition of RSA is presented in Table 1. The total percentage of oxides (SiO_2, Al_2O_3, and Fe_2O_3) in RSA was 75.4%. This value is higher than the minimum required value of 70% for using pozzolans. The RSA loss during the ignition was about 8.5%. This value is within the allowed value of 12% as a maximum percentage required for using pozzolans. It means that the RSA contains little unburned carbon, which is not pozzolanic material but used as filler to the mixture. The true density of RSA was 2.13 g/cm^3, which is less than the density of cement (3.15 g/cm^3), meaning that RSA is a lightweight material.

3.2. Bulk density

The bulk density of the RSA geopolymer adobe brick after a curing time of 28 days at different RSA and sodium hydroxide percentages is illustrated in Fig. 4a–c. The results in Table 3 showed a significant effect of RSA percentage and sodium hydroxide percentage on the bulk density of the RSA geopolymer adobe brick, where the bulk density decreases with the increase of RSA from 0% to 20%. The significant interaction between the bulk density and each of RSA and sodium hydroxide is shown in Fig. 4a–c and Table 4, which indicates that the maximum bulk density values were (~1.463 g/cm^3) at 0% RSA and 10% sodium hydroxide. In comparison, the minimum bulk density value was (~1.188 g/cm^3) at 20% RSA and 2.5% sodium hydroxide. The determined polynomial equations to calculate the bulk density of RSA geopolymer adobe brick are illustrated in Fig. 4a–c from the percentages of sodium hydroxide and RSA in the composite. The minimum, maximum, average, standard deviation, and standard error for the bulk density values are illus-

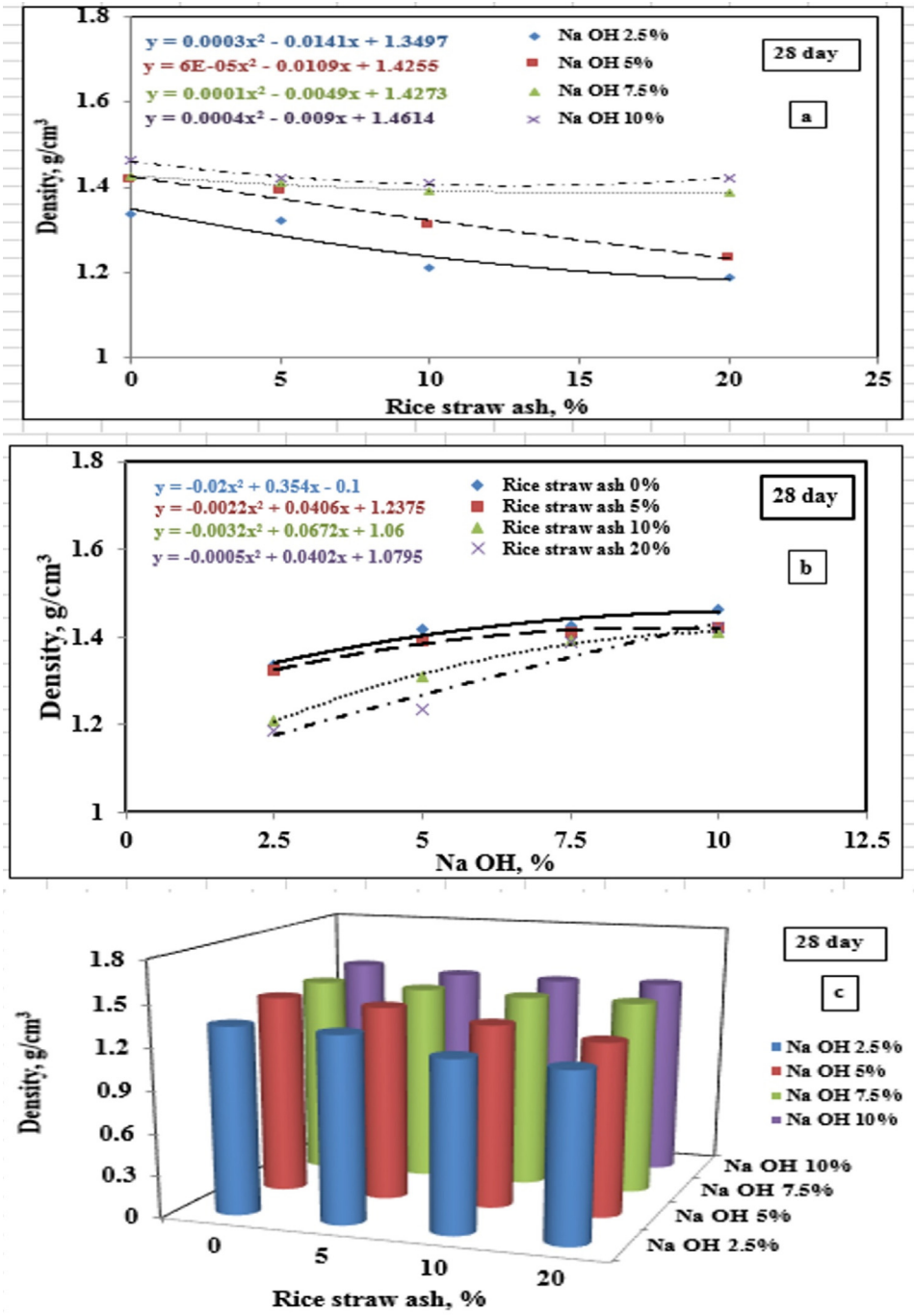

Fig. 4. Effect of RSA and sodium hydroxide percentage on the bulk density and the weight of the geopolymer adobe bricks after 28 days.

trated in Table 6. To make lightweight bricks, a geopolymer with 20% RSA and 10% sodium hydroxide is recommended, which decreases the bulk density and the weight of the bricks by about 30% from the conventional bricks.

3.3. Water absorption

The water absorption of hardened geopolymer adobe bricks after 28 days of hydration at different RSA and sodium hydroxide percentages is shown in Fig. 5a–c. The statistical analysis results in Table 3 showed a significant effect of RSA percentage and sodium hydroxide percentage on the water absorption of the RSA geopolymer adobe brick. Increasing RSA from 0% to 20% and sodium hydroxide from 2.5% to 10% decreased the water absorption of the geopolymer adobe bricks because of the reduction in the total porosity of the geopolymer sample. The significant interaction between water absorption and each of RSA and sodium hydroxide are shown in Fig. 5a–c and Table 4, which indicates that the maximum value of water absorption was (25.9%) at 10% RSA and 2.5% sodium hydroxide. In comparison, the minimum value was (8.3%) at 20% RSA and 10% sodium hydroxide. The minimum, maximum, average, standard deviation, and standard error of water absorption values are illustrated in Table 6. The geopolymer adobe brick samples comprising 0% RSA and 2.5%–7.5% sodium hydroxide and 5% RSA with 2.5% sodium hydroxide were dissolved in water after 28 days of hydration. Therefore, these RSA and

Table 3
Effects of RSA percentage and sodium hydroxide percentage on bulk density, weight, water absorption, thermal conductivity, and compressive strength of the geopolymer adobe bricks.

Treatments	Compressive strength (M.Pa) 7 day	Compressive strength (M.Pa) 28 day	Bulk density (g/cm^3)	Water absorption (%)	Weight (g)
A) RSA (%)					
0	0.95^{d}	1.18^{d}	1.41^{a}	5.13^{c}	361.22^{a}
5	1.21^{c}	1.32^{c}	1.39^{ab}	16.08^{a}	354.82^{ab}
10	1.40^{b}	1.65^{b}	1.33^{bc}	16.40^{a}	340.48^{bc}
20	1.46^{a}	1.75^{a}	1.31^{c}	13.03^{b}	334.85^{c}
$LSD_{0.05}$	0.05	0.06	0.06	0.64	14.49
B) Na OH (%)					
2.5	0.81^{d}	1.06^{d}	1.26^{c}	11.03^{b}	323.64^{c}
5.0	1.21^{c}	1.45^{c}	1.34^{b}	14.93^{a}	342.66^{b}
7.5	1.46^{b}	1.63^{b}	1.40^{a}	10.35^{c}	359.22^{b}
10.0	1.54^{a}	1.75^{a}	1.43^{a}	14.33^{a}	365.82^{a}
$LSD_{0.05}$	0.05	0.06	0.06	0.64	14.49
Interaction					
A × B	*	*	*	*	*

RSA: Rice straw ash.
Mean (s) in the same column had the same letter (s) are not significant.
*: significant difference at 0.05 level of probability.

Table 4
Interaction effects between RSA percentage and sodium hydroxide percentage on bulk density, weight, water absorption, thermal conductivity, and compressive strength of the geopolymer adobe bricks.

Treatments		Compressive strength (M.Pa) 7 day	Compressive strength (M.Pa) 28 day	Bulk density (g/cm^3)	Water absorption (%)	Weight (g)
A) RSA (%)	B) NaOH (%)					
0	2.5	0.50	0.65	1.34	0.00	342.02
	5.0	1.00	1.20	1.42	0.00	363.26
	7.5	1.10	1.40	1.43	0.00	365.06
	10.0	1.20	1.45	1.46	20.50	374.53
5	2.5	0.80	0.95	1.32	0.00	338.69
	5.0	1.20	1.33	1.39	25.80	355.84
	7.5	1.40	1.45	1.41	19.80	360.96
	10.0	1.45	1.56	1.42	18.70	363.78
10	2.5	0.93	1.30	1.21	25.90	309.76
	5.0	1.30	1.63	1.31	17.90	335.36
	7.5	1.65	1.75	1.39	12.00	355.84
	10.0	1.70	1.90	1.41	9.80	360.96
20	2.5	1.00	1.35	1.19	18.20	304.13
	5.0	1.35	1.64	1.24	16.00	316.16
	7.5	1.70	1.90	1.39	9.60	355.07
	10.0	1.80	2.10	1.42	8.30	364.03
$LSD_{0.05}$		0.11	0.13	0.12	1.28	28.98

RSA: Rice straw ash.

sodium hydroxide compositions are not recommended to manufacture the geopolymer adobe bricks.

3.4. Compressive strength (CS)

The compressive strength of the RSA geopolymer adobe bricks at 0%–20% RSA and 2.5%–10% sodium hydroxide after being hardened for 7 and 28 days are presented in Figs. 6 and 7(a–c), respectively. The results presented in Table 3 showed the significant effect of RSA percentage and sodium hydroxide percentage on the compressive strength of the RSA geopolymer adobe bricks after 7 and 28 days. The compressive strength for all tested hardened geopolymer adobe bricks increases with the increase in RSA from (0% to 20%) and sodium hydroxide from (2.5% to 10%) because of the transformation of the amorphous silica to geopolymer network due to the pozzolanic reaction between RSA and sodium hydroxide, which increases the bonding efficiency of RSA with the soil. Moreover, the CS after 28 days was higher than after 7 days for all specimens by ~20–30%, which is due to an increase in the CS with curing time. The significant interaction between compressive strength and each of RSA and sodium hydroxide are shown in Figs. 6 and 7(a–c) and Table 4, which indicates that the maximum values of CS were (1.8 and 2.1 MPa) after 7 and 28 days of curing, respectively, at the best condition of sodium hydroxide (10%) and RSA (20%). In contrast, the minimum values were (0.5 and 0.65 MPa) after 7 and 28 days of curing, respectively, at 0% RSA and 2.5% sodium hydroxide. The determined polynomial equations are illustrated in Figs. 6, 7a and b to calculate the CS of RSA geopolymer adobe bricks for different percentages of sodium hydroxide and RSA after curing times of 7 and 28 days, respectively. The minimum, maximum, average, standard deviation, and standard error of the compressive strength values are illustrated in Table 6. It was observed that the CS of RSA geopolymer adobe bricks are low compared to other types of concrete due to increasing the porosity and the voids in the composite, which contributed to decreased thermal conductivity and weight the bricks. Using RSA geopolymer adobe bricks on building interior walls at the maximum CS of (2.1 MPa) after 28 days is recommended.

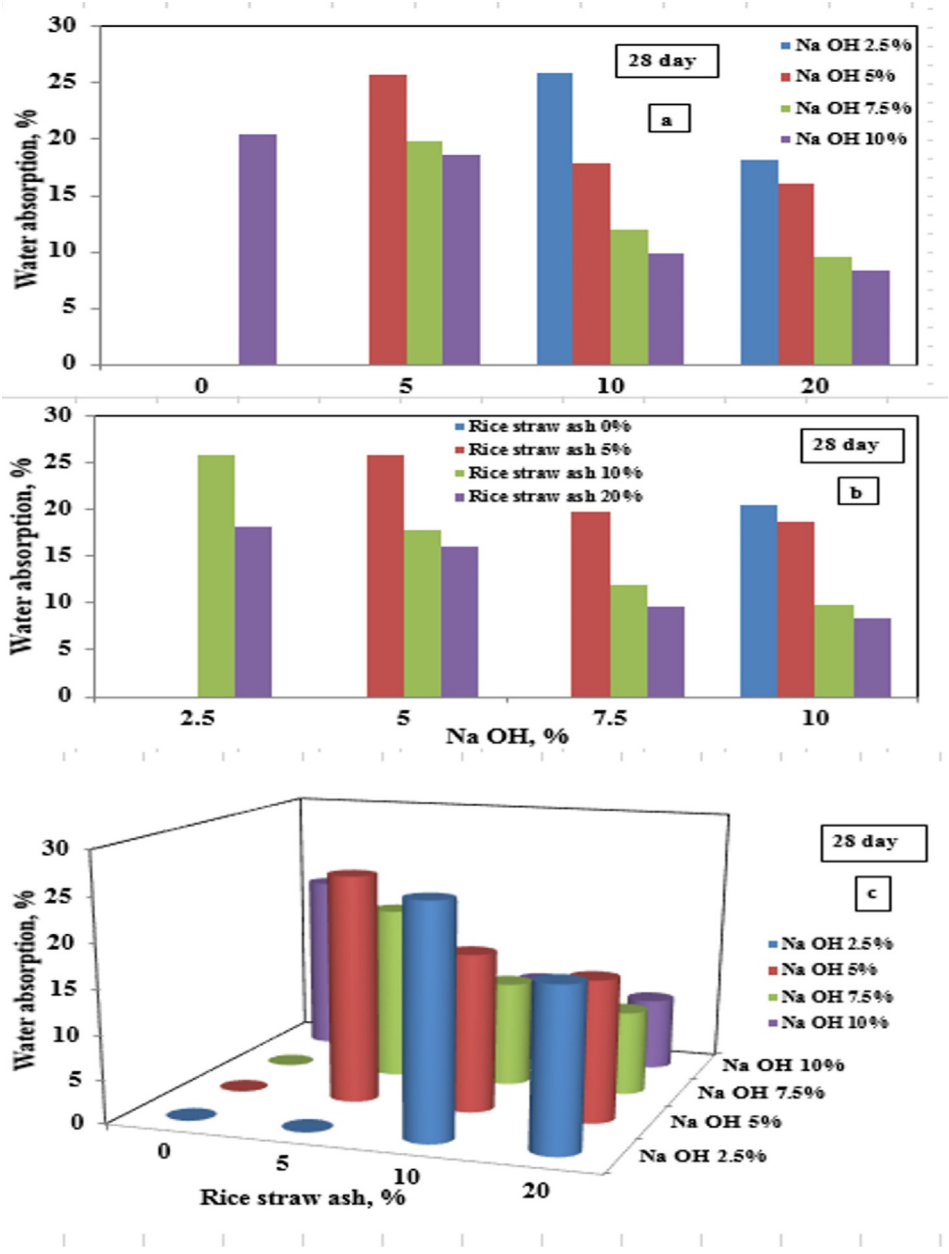

Fig. 5. Effect of RSA and sodium hydroxide on the water absorption of the geopolymer adobe bricks after 28 days.

3.5. Thermal conductivity

The thermal conductivity of geopolymer adobe brick was measured at different percentages of RSA (0–20%) and the highest sodium hydroxide percentage of 10% because that is the best percentage to maximize the CS and minimize the water absorption and weight of the geopolymer adobe bricks as shown in Fig. 8. Data in Table 5 showed that the RSA percentage significantly affected the thermal conductivity, which decreases with the increase in RSA percentage because the thermal conductivity of RSA is lower than that of the soil sample. The maximum thermal conductivity was (0.87 W/(m·K)) at 5% RSA and 10% sodium hydroxide, whereas the minimum thermal conductivity was (0.46 W/(m·K)) at 20% RSA and 10% sodium hydroxide. The thermal conductivity decreases with the increase in RSA percentage because the thermal conductivity of RSA is lower than the soil. Still, at RSA of 5%, the effect of rice straw ash was not so great to decrease the thermal conductivity and the effect of the standard error of the thermal conductivity values as illustrated in Table 6. The minimum, maximum, average, standard deviation, and standard error of the thermal conductivity values are illustrated in Table 6. The determined polynomial equation to calculate the thermal conductivity of RSA geopolymer adobe brick at different percentages of RSA is illustrated in Fig. 8.

3.6. Characteristics of the composite

3.6.1. A. Scanning electronic microscopy (SEM)

SEM state-of-the-art analysis provides an enlarged image of the size, shape, composition, crystallography, and surface structures. It evaluates the differences in the surface and other physical and chemical characteristics of a specimen. The SEM images of soil, RSA, and different hardened samples are displayed in Fig. 9a–e. The SEM image for RSA revealed that most RSA particles are irreg-

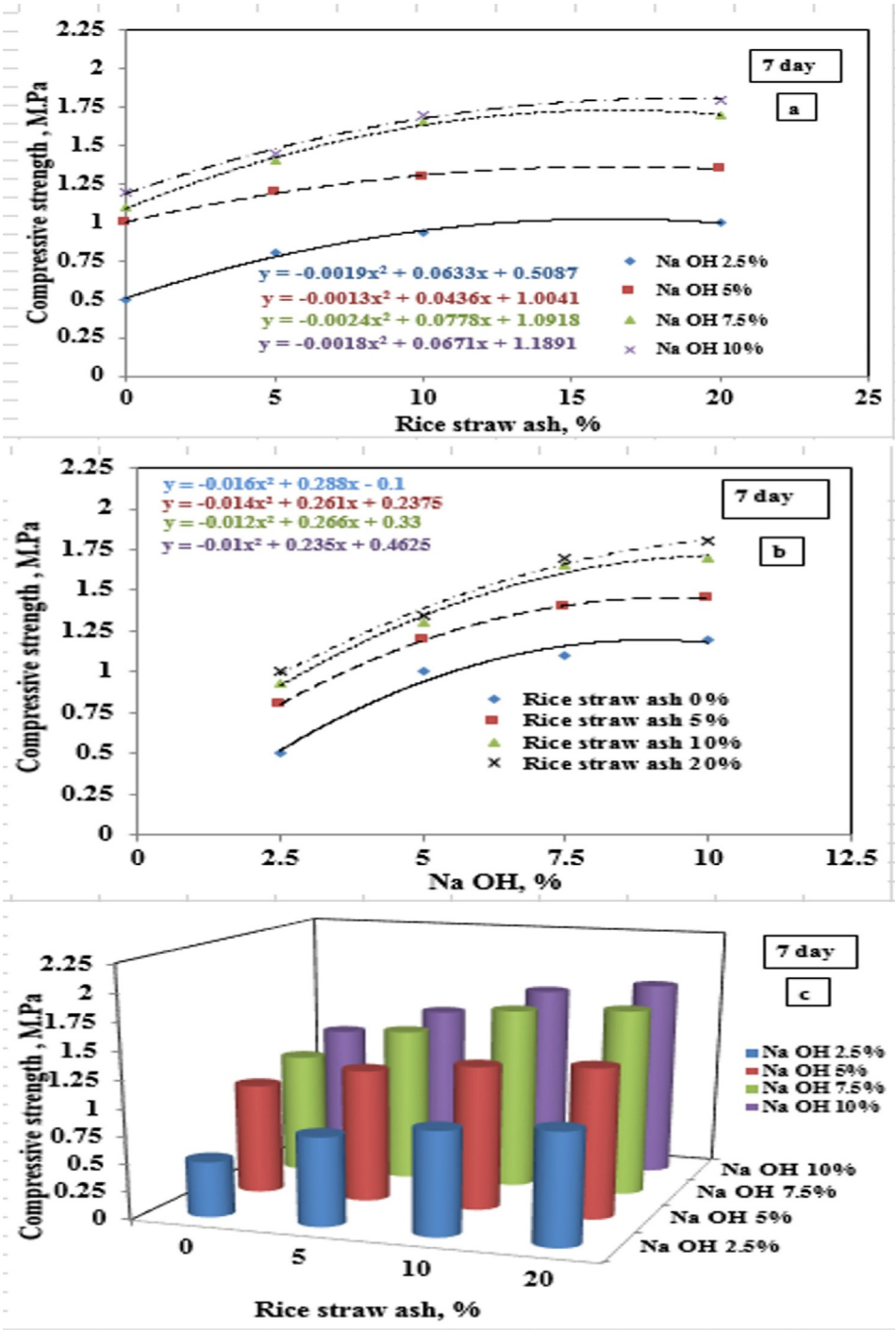

Fig. 6. Effect of RSA and sodium hydroxide percentage on the compressive strength of the geopolymer adobe bricks after 7 days.

ular in shape, with an amorphous and porous surface (Fig. 9a). Some RSA particles also have a smooth surface. The reactivity of pozzolanic material is endorsed to its high content of amorphous silica and porous nature. SEM images of the soil sample display a loose and unconnected form (Fig. 9b). The soil particles are regular in shape, crystallized, and have a rough and hemispherical surface. The SEM image of the soil sample with sodium hydroxide is displayed in Fig. 9c. The soil particles are coated with a white surface because of the soil and sodium hydroxide reaction. The SEM image of the soil sample with sodium hydroxide and sodium silicate appears interconnected, as shown in Fig. 9d. The SEM image of RSA geopolymer adobe brick is shown in Fig. 9e.

3.6.2. Ftir spectroscopy

The FTIR spectra for soil, RSA, and geopolymer adobe brick were attained to identify the structure of the material and the type of bonds or functional groups as displayed in Fig. 10a–c. 1-The FTIR spectrum for the soil sample as presented in Fig. 10a has a strong and significant band at 3473 cm^{-1} assigned to the —OH stretching vibration in the soil, which is assigned to the HO—H stretching vibrations that might be attributed to chemisorbed water as well as hydroxyl group peaks at 1802, 873, and 713 cm^{-1} pertaining the CO_3 group which reveals a combination of calcite and dolomite, which is not separable. The peak at 713 cm^{-1} is indicative of calcite. 2-The FTIR spectrum for the RSA sample in Fig. 10b. Zone 1

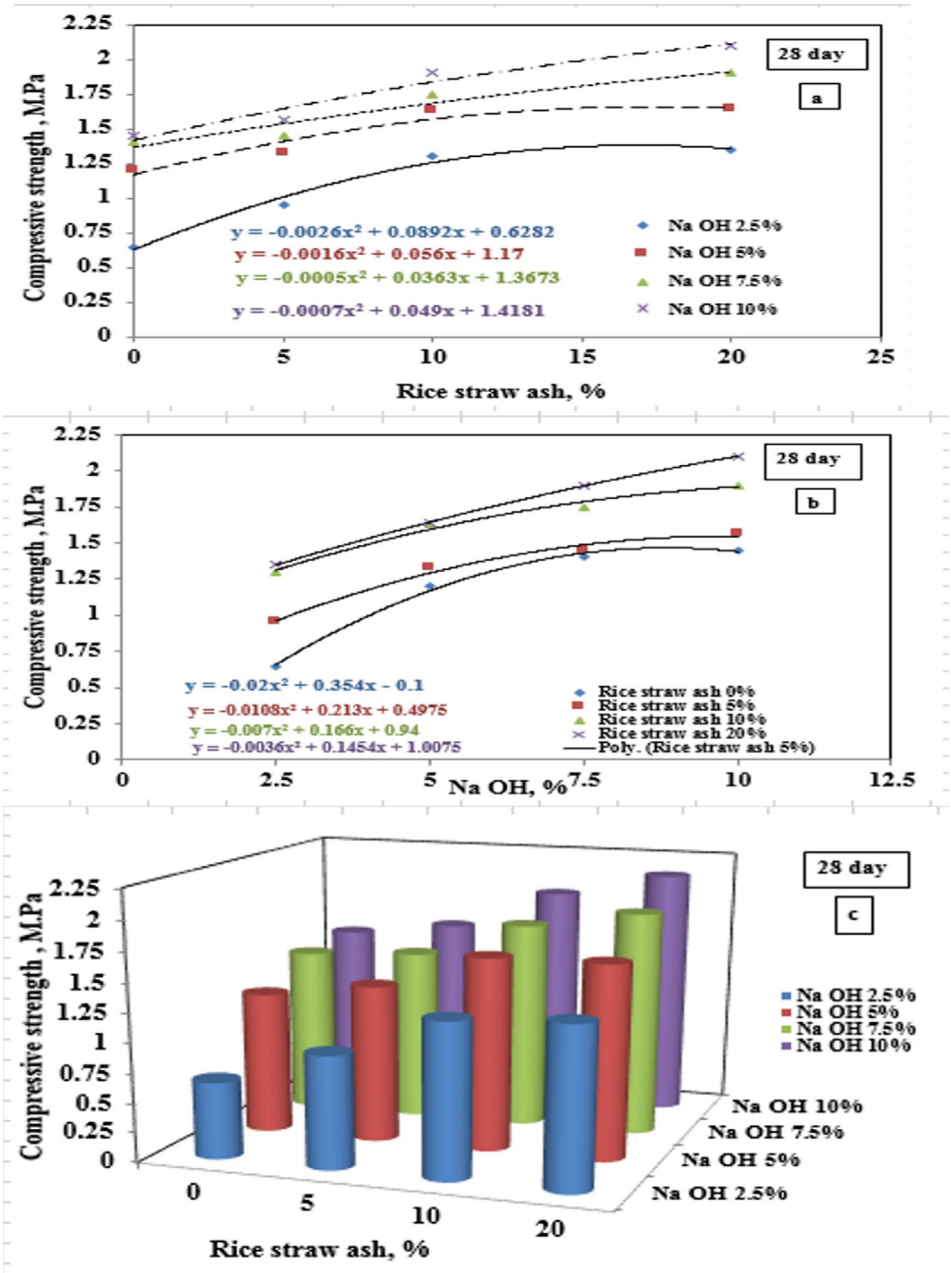

Fig. 7. Effects of RSA and sodium hydroxide on the compressive strength of the geopolymer adobe bricks after 28 days.

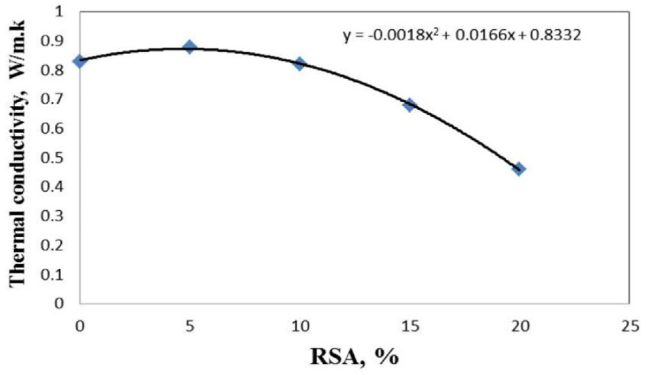

Fig. 8. Effect of RSA on the thermal conductivity of the geopolymer adobe bricks.

Table 5
Effects of RSA percentage on the thermal conductivity of the geopolymer adobe bricks.

RSA (%)	Thermal conductivity (W/m·k)
0	0.83 [a]
5	0.88 [a]
10	0.82 [a]
15	0.68[b]
20	0.46[c]
LSD $_{0.05}$	0.068

RSA: Rice straw ash.
Mean (s) in the same column had the same letter (s) are not significant.

Table 6
The minimum, maximum, average, standard deviation, and standard error for bulk density, weight, water absorption, thermal conductivity, and compressive strength of the geopolymer adobe bricks.

Characteristic	Compressive strength (MPa) 7 day	Compressive strength (MPa) 28 day	Bulk density (g/cm^3)	Water absorption (%)	Weight (g)	Thermal conductivity (W/m·k)
Minimum	0.48	0.62	1.18	8.3	288.92	0.46
Maximum	1.8	2.1	1.46	25.9	393.25	0.87
Average	1.26	1.47	1.36	12.66	347.84	0.73
Standard Deviation	0.36	0.36	0.10	8.93	25.47	0.16
Standard error	0.05	0.05	0.01	1.29	3.68	0.04

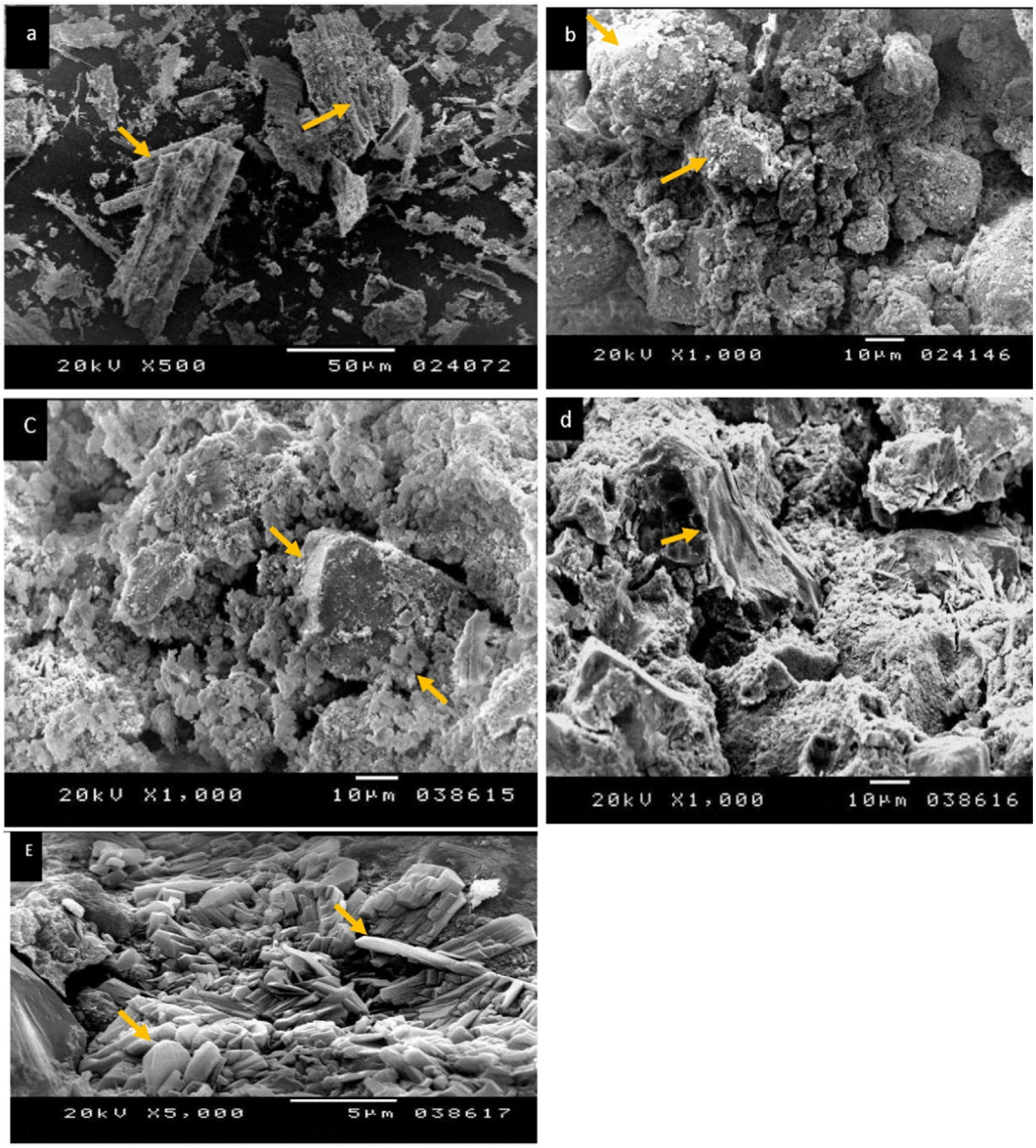

Fig. 9. SEM images of soil, RSA, and different hardened samples (a–e).

(approximately 3500–3000 cm^{-1}) signifies the symmetric and asymmetric —OH stretching vibrations trapped–OH. Zone 2 (1092–796 cm^{-1}) indicates vibration due to H—O—H bending, where there is the characteristic band of the silica bond with oxygen. Further, the characteristic bands for Si—O and Si—O—Si at 1092 and 796 cm^{-1}, respectively, are observed. Bands close to 500 cm^{-1} are related to the metal–oxygen (silicon). The FTIR spectrum for RSA geopolymer adobe brick in Fig. 10c illustrates a strong peak at 1031 cm^{-1}, attributed to the vibration stretching of Si—O—Si, which confirms the existence of silicate (referred to as sodium silicate). The significant peak at 1798 cm^{-1} is due to the CO_3 in calcite and dolomite, in general, we can observe C═O stretching. Further, the changes in the spectra of the soil sample due to the addition RSA and alkaline activators are observed. The stretched bands at 350–1200 cm^{-1} are attributed to the phase change of RSA due to geopolymerization. These bands display the

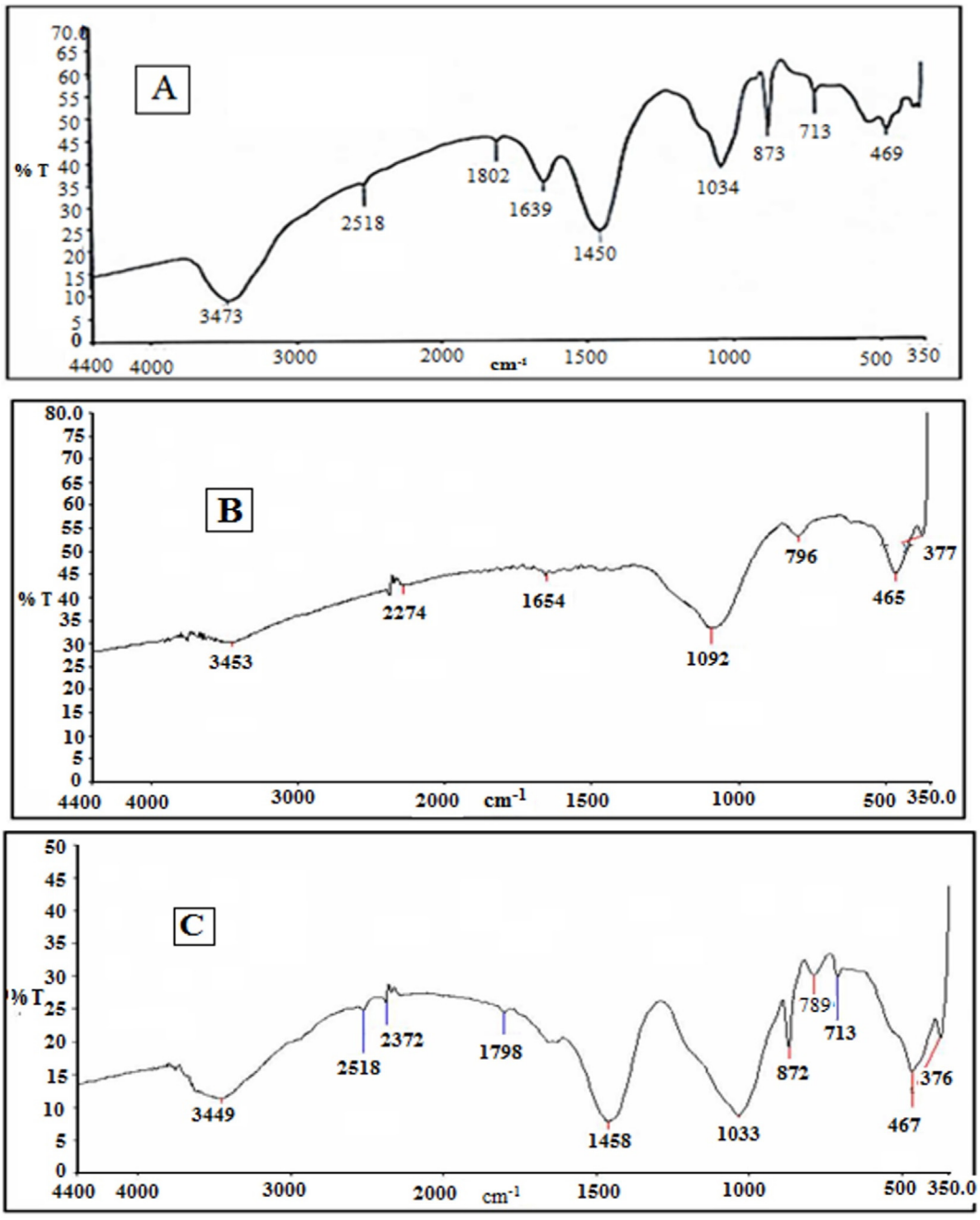

Fig. 10. Fourier transform infrared spectra. (a) soil, (b) rice straw ash and (c) rice straw ash geopolymer adobe brick.

behavior of moving to the right or moving to lower wave numbers from the untreated to treated soil caused by geopolymerization.

4. Discussion

During this study, the RSA geopolymer adobe bricks were manufactured and tested at different percentages of RSA (0%, 5%, 10%, and 20%) and sodium hydroxide (2.5%, 5%, 7.5%, and 10%) by measuring the bulk density, water absorption, compressive strength, and thermal conductivity after a curing time of 28 days to produce low thermal conductivity and moisture-resistant geopolymer lightweight adobe bricks with maximum compressive strength.

The bulk density of the RSA geopolymer adobe brick after curing time of 28 days at different percentages of RSA and sodium hydroxide showed a significant effect. This is because the bulk density of RSA is lower than the soil and the increase in voids in the geopolymer adobe brick matrix as the percentage of RSA increases, as reported by Morsy and Mohamed (2018) and El-Sayed and Shaheen (2020).

However, the bulk density increases with the sodium hydroxide percentage from 2.5% to 10%. This is because of the transformation of the amorphous silica to geopolymer network that increases the cohesion of the soil with RSA, thereby decreasing the voids in the RSA geopolymer adobe bricks and these findings agree with (de Castrillo et al., 2021; Ige and Danso, 2021; Trang et al., 2021).

The bulk density and weight of the normal solid concrete brick with the same dimensions of 40 × 40 × 160 mm^3 were about (2 g/cm^3) and (512 g) respectively, according to Oti et al. (2009, 2010) and Abdeldjalil and Yousfi (2020).

The statistical analysis showed a significant effect of RSA % and sodium hydroxide % on the water absorption of the RSA geopoly-

mer adobe brick, and these results agree with (Tai et al., 2020; Hany et al., 2021). According to Lertwattanaruk and Choksiriwanna (2011), the lightweight concrete brick is continuous absorb the moisture until the humidity of the brick reach 70% therefore, 20% RSA and 10% sodium hydroxide is the best condition to produce moisture-resisting geopolymer adobe bricks with water absorption of (8.3%).

The results showed a significant effect of RSA percentage and sodium hydroxide percentage on the compressive strength of the RSA geopolymer adobe bricks after 7 and 28 days as reported before by Roselló et al. (2017) and Morsy and Mohamed (2018). Moreover, the CS after 28 days was higher than that after 7 days for all specimens by ~20–30%, which is due to an increase in the CS with curing time as reported by Fernández-Jiménez and Palomo (2003).

Therefore, to decrease the thermal conductivity of the geopolymer adobe bricks, additives of 20% RSA are recommended to use in the sample. Reducing the thermal conductivity of the adobe brick is essential to increase its insulation and sound-absorbing capacities for inner walls, which decrease the energy demands of heating and cooling systems (Khorsand et al., 2013; Roselló et al., 2017; Hany et al., 2021).

In the current results, Crusts appear on the surface of the soil particles, indicating complete interconnection between soil particles and RSA. This is due to the transformation of the amorphous silica to a geopolymer network because of the pozzolanic reaction between RSA and sodium hydroxide and these results agree with those (Berger, 2010; Lertwattanaruk and Choksiriwanna, 2011; Tome et al., 2021).

The soil used for geopolymer adobe brick formulation has a good geotechnical and there is a significant effect of RSA on all studied characters. The main results indicated that increasing RSA from 0% to 20% decreases the bulk density, water absorption, thermal conductivity, and increased compressive strength. Therefore, in future buildings design, it could be useful to use adobes bricks, a construction material adobe mixed with 20% RSA and 10% sodium hydroxide could be efficient to produce low thermal conductivity and moisture-resistant geopolymer lightweight adobe bricks with maximum compressive strength as reported by Piyaphanuwat and Asavapisit (2009), Oti et al. (2010), Lertwattanaruk and Choksiriwanna (2011) and Yuan et al. (2014).

5. Conclusions

Rice straw ash waste was used as a stabilizing material with sodium hydroxide to produce geopolymer adobe brick at different percentages of RSA (0%, 5%, 10%, and 20%) and sodium hydroxide (2.5%, 5%, 7.5%, and 10%). The new composite samples were tested by measuring the bulk density, water absorption, thermal conductivity, and compressive strength after a curing time of 28 days to obtain good quality geopolymer adobe bricks. The results obtained show that (1) the soil used for geopolymer adobe brick formulation has a good geotechnical and particle size characteristics; (2) the statistical analysis showed a significant effect of RSA percentage sodium hydroxide percentage and their interaction on all studied characters; (3) increasing RSA from 0% to 20% decreased the bulk density, water absorption, and thermal conductivity and increased the compressive strength; (4) increasing sodium hydroxide from 2.5% to 10% increased the bulk density and the compressive strength, while resulting in decreased water absorption; (5) the maximum value of compressive strength was 2.1 MPa after 28 days of curing at 20% RSA and 10% sodium hydroxide, these adobes bricks can be used on a non-load-bearing wall, so it is recommended to use RSA geopolymer adobe bricks for interior walls; (6) the minimum value of water absorption and thermal conductivity was 8.3% and 0.46 W/(m·K), respectively, at 20% RSA and 10% sodium hydroxide so it can be used as low thermal conductivity and moisture-resistant materials; (7) the minimum values of bulk density and weight were about 1.188 g/cm^3 and 304.1 g at 20% RSA and 2.5% sodium hydroxide 2.5%. Using 20% RSA and 10% sodium hydroxide decrease the bulk density and the weight of the brick by ~30%; (8) therefore, in the design of future buildings using adobes bricks, a construction material adobe mixed with 20% RSA and 10% sodium hydroxide could be efficient to produce low thermal conductivity and moisture-resistant geopolymer lightweight adobe bricks with maximum compressive strength.

Declaration of Competing Interest

The authors declare that they have no known competing financial interests or personal relationships that could have appeared to influence the work reported in this paper.

Acknowledgements

The authors extend their appreciation to the deanship of Scientific Research at King Khalid University, Abha KSA for supporting this work under grant number (R.G.P./78/41).

References

Abdeldjalil, M., Yousfi, S., 2020. Identification of sands of dune and concretes using a granular model-Case of arid region. Case Stud. Constr. Mater. 13, e00458.
Ahmari, S., Zhang, L., 2012. Production of eco-friendly bricks from copper mine tailings through geopolymerization. Constr. Build. Mater. 29, 323–331.
Alvarado, S., Marín, E., Juárez, A., Calderón, A., Ivanov, R., 2012. A hot-wire method based thermal conductivity measurement apparatus for teaching purposes. Euro. J. Phys. 33, 897.
Arshad, M.S., Pawade, P., 2014. Reuse of natural waste material for making light weight bricks. Int. J. Sci. Technol. Res. 3, 49–53.
ASTM, D., 1950. American society for testing and materials (ASTM). American Association of State Highway and Transportation Officials-AASHTO Standards, United States.
Babé, C., Kidmo, D.K., Tom, A., Mvondo, R.R.N., Boum, R.B.E., Djongyang, N., 2020. Thermomechanical characterization and durability of adobes reinforced with millet waste fibers (sorghum bicolor). Case Stud. Constr. Mater. 13, e00422.
Bamminger, C., Poll, C., Marhan, S., 2018. Offsetting global warming-induced elevated greenhouse gas emissions from an arable soil by biochar application. Global Change Biol. 24, e318–e334.
Berger, M.B., 2010. The importance and testing of density/porosity/permeability/pore size for refractories. In: The Southern African Institute of Mining and Metallurgy Refractories Conference. pp. 101–116.
Bondar, D., Lynsdale, C., Milestone, N.B., Hassani, N., Ramezanianpour, A.A., 2011. Effect of type, form, and dosage of activators on strength of alkali-activated natural pozzolans. Cem. Concr. Compos. 33, 251–260.
Buyondo, K.A., Olupot, P.W., Kirabira, J.B., Yusuf, A.A., 2020. Optimization of production parameters for rice husk ash-based geopolymer cement using response surface methodology. Case Stud. Constr. Mater. 13, e00461.
Capson-Tojo, G., Moscoviz, R., Astals, S., Robles, Á., Steyer, J.-P., 2020. Unraveling the literature chaos around free ammonia inhibition in anaerobic digestion. Renew. Sust. Energy Rev. 117, 109487.
de Castrillo, M.C., Ioannou, I., Philokyprou, M., 2021. Reproduction of traditional adobes using varying percentage contents of straw and sawdust. Constr. Build. Mater. 294, 123516.
Dirgantara, R., Gunasekara, C., Law, D.W., Molyneaux, T.K., 2017. Suitability of brown coal fly ash for geopolymer production. J. Mater. Civil Eng. 29, 04017247.
Duncan, D.B., 1955. Multiple range and multiple F tests. Biometrics 11, 1–42.
El-Sayed, T.A., Shaheen, Y.B., 2020. Flexural performance of recycled wheat straw ash-based geopolymer RC beams and containing recycled steel fiber. Struct. Elsevier, 1713–1728.
Fernández-Jiménez, A., Palomo, A., 2003. Characterisation of fly ashes. Potential reactivity as alkaline cements☆. Fuel 82, 2259–2265.
Foaud, A., Abdelradi, F., 2016. Analysis of the rice straw recycling value added in egypt agricultural economics. J. Agric. Econom. Soc. Sci. Mansoura .Univ. 11, 1039–1045.
Gavali, H.R., Bras, A., Ralegaonkar, R.V., 2021. Cleaner construction of social housing infrastructure with load-bearing alkali-activated masonry. Clean Technol. Environ. Policy, 1–16.
Gomez, K.A., Gomez, A.A., 1984. Statistical Procedures for Agricultural Research. John Wiley & Sons.
Gunasekara, C., Setunge, S., Law, D.W., Willis, N., Burt, T., 2018. Engineering properties of geopolymer aggregate concrete. J. Mater. Civil Eng. 30, 04018299.

Habert, G., Billard, C., Rossi, P., Chen, C., Roussel, N., 2010. Cement production technology improvement compared to factor 4 objectives. Cem. Concr. Res. 40, 820–826.
Habert, G., De Lacaillerie, J.D.E., Roussel, N., 2011. An environmental evaluation of geopolymer based concrete production: reviewing current research trends. J. Clean. Prod. 19, 1229–1238.
Hansen, T.C., Boegh, E., 1985. Elasticity and drying shrinkage concrete of recycled-aggregate. J. Proc., 648–652
Hany, E., Fouad, N., Abdel-Wahab, M., Sadek, E., 2021. Investigating the mechanical and thermal properties of compressed earth bricks made by eco-friendly stabilization materials as partial or full replacement of cement. Constr. Build. Mater. 281, 122535.
Hassan, M.K., Chowdhury, R., Ghosh, S., Manna, D., Pappinen, A., Kuittinen, S., 2021. Energy and environmental impact assessment of Indian rice straw for the production of second-generation bioethanol. Sust. Energy Technol. Assess. 47, 101546.
Ige, O., Danso, H., 2021. Physico-mechanical and thermal gravimetric analysis of adobe masonry units reinforced with plantain pseudo-stem fibres for sustainable construction. Constr. Build. Mater. 273, 121686.
Ismail, H., Shamsudin, R., Azmi, M., Hamid, A., Awang, R., 2016. Characteristics of β-wollastonite derived from rice straw ash and limestone. J. Austr. Ceram. Soc. 52, 163–174.
Jiang, M., Chen, X., Rajabipour, F., Hendrickson, C.T., 2014. Comparative life cycle assessment of conventional, glass powder, and alkali-activated slag concrete and mortar. J. Infrastruct. Syst. 20, 04014020.
Jullien, A., Proust, C., Martaud, T., Rayssac, E., Ropert, C., 2012. Variability in the environmental impacts of aggregate production. Resour. Conserv. Recycl. 62, 1–13.
Kalapathy, U., Proctor, A., Shultz, J., 2002. An improved method for production of silica from rice hull ash. Bioresour. Technol. 85, 285–289.
Khodr, M., Law, D.W., Gunasekara, C., Setunge, S., Brkljaca, R., 2020. Compressive strength and microstructure evolution of low calcium brown coal fly ash-based geopolymer. J. Sust. Cem.-Based Mater. 9, 17–34.
Khorsand, H., Kiayee, N., Masoomparast, A.H., 2013. Optimization of amorphous silica nanoparticles synthesis from rice straw ash using design of experiments technique. Particul. Sci. Technol. 31, 366–371.
Kubiś, M., Pietrak, K., Cieślikiewicz, Ł., Furmański, P., Wasik, M., Seredyński, M., Wiśniewski, T.S., Łapka, P., 2020. On the anisotropy of thermal conductivity in ceramic bricks. J. Build. Eng. 31, 101418.
Kurmus, H., Mohajerani, A., 2021. Energy savings, thermal conductivity, micro and macro structural analysis of fired clay bricks incorporating cigarette butts. Constr. Build. Mater. 283, 122755.
Lertwattanaruk, P., Choksiriwanna, J., 2011. The physical and thermal properties of adobe brick containing bagasse for earth construction. Int. J. Build. Urban Inter. Landscape Technol. (BUILT) 1, 57–66.
Li, Z., Ding, Z., Zhang, Y., 2004. Development of sustainable cementitious materials, in: Proceedings of International Workshop on Sustainable Development and Concrete Technology, Beijing, China, pp. 55–76.
Mohamed, H., Morsy, M., 2018. Study the effect of dry fermentation of goat manure in optimization of biogas production and minimization of costs. Misr J. Agric. Eng. 35, 1149–1164.
Mohamed, H., Morsy, M., 2020. The fine grinding of corncobs to use as a water absorption material. Misr J. Agric. Eng. 37, 165–184.
Morsy, M., Mohamed, H., 2018. Experimental investigation on some parameters of rice straw ash-fly ash geopolymer mortar. Misr J. Agric. Eng. 35, 1083–1098.
Nan, Q., Yi, Q., Zhang, L., Ping, F., Thies, J.E., Wu, W., 2020. Biochar amendment pyrolysed with rice straw increases rice production and mitigates methane emission over successive three years. Waste Manage. 118, 1–8.
Nanayakkara, O., Gunasekara, C., Sandanayake, M., Law, D.W., Nguyen, K., Xia, J., Setunge, S., 2021. Alkali activated slag concrete incorporating recycled aggregate concrete: Long term performance and sustainability aspect. Constr. Build. Mater. 271, 121512.
Nanda, S., Mohanty, P., Pant, K.K., Naik, S., Kozinski, J.A., Dalai, A.K., 2013. Characterization of North American lignocellulosic biomass and biochars in terms of their candidacy for alternate renewable fuels. Bioenergy Res. 6, 663–677.
Oti, J., Kinuthia, J., Bai, J., 2009. Compressive strength and microstructural analysis of unfired clay masonry bricks. Eng. Geol. 109, 230–240.
Oti, J., Kinuthia, J., Bai, J., 2010. Design thermal values for unfired clay bricks. Mater. Des. 31, 104–112.
Phuong, P.-T.-H., Nghiem, T.-D., Thao, P.-T.-M., Pham, C.-T., Thi, T.-T., Dien, N.T., 2021. Impact of rice straw open burning on local air quality in the Mekong Delta of Vietnam. Atmosph. Pollut. Res. 12, 101225.
Piyaphanuwat, R., Asavapisit, S., 2009. Effect of black rice husk ash substituted OPC on strength and leaching of solidified plating sludge. J. Metals Mater. Min. 19.
Roselló, J., Soriano, L., Santamarina, M.P., Akasaki, J.L., Monzó, J., Payá, J., 2017. Rice straw ash: a potential pozzolanic supplementary material for cementing systems. Ind. Crops Prod. 103, 39–50.
Tai, W., He, L., Zhang, X., Pu, J., Voronin, D., Jiang, S., Zhou, Y., Du, L., 2020. Characterization of the receptor-binding domain (RBD) of 2019 novel coronavirus: implication for development of RBD protein as a viral attachment inhibitor and vaccine. Cell. Mol. Immunol. 17, 613–620.
Thomas, B.S., Yang, J., Mo, K.H., Abdalla, J.A., Hawileh, R.A., Ariyachandra, E., 2021. Biomass ashes from agricultural wastes as supplementary cementitious materials or aggregate replacement in cement/geopolymer concrete: a comprehensive review. J. Build. Eng. 102332.
Tome, S., Nana, A., Kaze, C.R., Djobo, J.N.Y., Alomayri, T., Kamseu, E., Etoh, M.-A., Etame, J., Kumar, S., 2021. Resistance of alkali-activated blended volcanic Ash-MSWI-FA mortar in sulphuric acid and artificial seawater. Silicon, 1–8.
Trang, N.T.M., Ho, N.A.D., Babel, S., 2021. Reuse of waste sludge from water treatment plants and fly ash for manufacturing of adobe bricks. Chemosphere 284, 131367.
Yuan, Q., Pump, J., Conrad, R., 2014. Straw application in paddy soil enhances methane production also from other carbon sources. Biogeosciences 11, 237–246.
Yusuf, A.A., Inambao, F.L., Hassan, A.S., Nura, S.S., Karthickeyan, V., 2020. Comparative study on pyrolysis and combustion behavior of untreated Matooke biomass wastes in East Africa via TGA, SEM, and EDXS. Int. J. Energy Environ. Eng. 11, 265–273.
Zhang, X., Bai, C., Qiao, Y., Wang, X., Jia, D., Li, H., Colombo, P., 2021. Porous geopolymer composites: a review. Compos. Part A: Appl. Sci. Manuf., 106629